Full-Scale Demonstration of Higher Harmonic Control for Noise and Vibration Reduction on the XV-15 Rotor

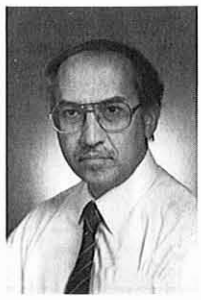

Khanh Nguyen Mark Betzina Cahit Kitaplioglu

Aerospace Engineers

Army/NASA Rotorcraft Division, NASA Ames Research Center, Moffett Field, CA

A higher harmonic control (HHC) investigation was conducted on a full-scale, isolated XV-15 rotor in helicopter mode in the NASA Ames 80- by 120-Foot Wind Tunnel to independently control noise and vibration. The higher harmonic blade pitch was generated using swashplate oscillations. The radiated blade-vortex interaction (BVI) noise footprint was measured on a plane beneath the rotor with an acoustic traverse. Test results showed that HHC is highly effective in reducing BVI noise, achieving a 12 dB reduction in peak noise level within the noise footprint. Noise reduction with HHC remains effective even with perturbations in rotor trim and flight conditions. Blade pressure feedback was demonstrated to be a viable method for closed-loop noise control. Some noise reduction was achieved with no increase in vibratory hub loads. Increases in control loads due to HHC generally limited further noise reduction. The vibration controller achieved about 50 percent reduction in vibratory hub loads with control loads limiting the HHC amplitude.

Introduction

Tiltrotor aircraft, employing swiveling rotors that allow the aircraft to take-off and land like helicopters but also fly like propeller airplanes, have great potential to relieve airport congestion. These aircraft have been proposed to ferry passengers directly to and from vertiports located near urban areas and mass transit. However, such a proposal has been hampered by concerns over the noise levels generated by these aircraft during landing approach (Ref. 1). Furthermore, tiltrotors operated in edgewise flight can generate higher vibration levels than helicopters due to the stiff-inplane blades (Ref. 2). The development of low-noise, low-vibration tiltrotors is essential in the success of this new mode of air transportation and greatly expands the utility of tiltrotor aircraft.

As a rotor descends into its own wake during landing approach, large air pressure fluctuations are generated on the rotor blades as each blade interacts with the tip vortices generated previously. The parallel blade-vortex interactions (BVI) are the source of the distinctly impulsive noise radiated from rotor blades. Tiltrotors can generate significantly higher noise than helicopters due to higher blade loading. Blade vortex interaction noise is a community disturbance that severely restricts civilian operations of rotorcraft in populated areas and is a source of early detection in military operations (Ref. 3).

While passive noise reduction methods can reduce BVI noise, they can impose severe penalties on the aircraft performance, the aircraft empty weight, or the rotor structural loads. Classical passive methods for noise reduction employ rotor solidity (blade chord or blade number) to reduce blade loading, blade tip shape to reduce tip vortex strength, or reduced rotor tip speed (Ref. 4). Recently, wind tunnel tests of the ERATO model rotor with a non-traditional blade planform has demonstrated significant noise reduction, up to 7 dB compared to a more traditional reference rotor in equivalent BVI conditions (Ref. 5). Besides the noise benefits, the ERATO rotor exhibited better rotor performance than the reference rotor but had some setbacks due to blade structural loads.

The development of low-noise approach profiles has shown potential for noise reduction of tiltrotor aircraft. By exploiting the nacelle-tilt and wing-flap settings, several approach profiles flight-tested on the XV-15 aircraft have shown up to 7 dB in noise reduction (Ref. 6) compared to a baseline profile. Operational methods offer an additional benefit since they can be used along with low-noise rotor designs to yield larger noise reduction.

In addition to passive methods and approach operations, methods using active blade pitch also have potential to reduce rotorcraft noise. In particular, higher harmonic control (HHC) has been shown to be effective in reducing BVI noise on helicopters. In this method, the swashplate was excited with dynamic actuators at the blade-number (N) harmonic, resulting in blade pitch oscillations at $N-1$, N, and $N+1$ per-rev (P) in the rotating frame. Up to 6 dB in BVI noise reductions were reported independently by Brooks (Ref. 7) and Splettstoesser (Ref. 8) on two different model rotors using HHC. In both cases, noise reduction was accompanied by increases in vibratory hub loads. These test results led to the formation of the Higher-harmonic Aeroacoustic Rotor Test (HART), a multi-national cooperative research program aimed at exploring the physics of noise and vibration reduction with HHC. The HART has been conducted on a BO-105 model rotor in the DNW wind tunnel (Ref. 9). In addition to the wind tunnel tests, HHC benefits were also demonstrated in flight on a research Gazelle helicopter, achieving 3.5 EPNdB (Effective Perceived Noise) in BVI noise reduction (Ref. 10).

Besides noise control, HHC has been proposed as a control method for helicopter vibration. The HHC input generates the higher harmonic airloads to suppress the oscillatory blade loads that cause airframe vibration. Compared to passive vibration control devices, HHC offers many benefits including better performance, weight savings, and robustness to changes in flight conditions. Results from both flight (Refs. 11–13) and

Presented at the American Helicopter Society 56th Annual Forum, Virginia Beach, VA, May 2–4, 2000. Manuscript received March 2000; accepted February 2001.

wind tunnel tests (Refs. 14, 15) demonstrated that HHC was very effective in suppressing helicopter vibration. A recent wind tunnel test of a semispan V-22 scaled model showed that HHC could be used to reduce tiltrotor-induced vibration in airplane mode (Ref. 16).

Individual-blade-control (IBC) is another active control method that has potential to reduce both noise and vibration on helicopters. In this method, the pitch-links are replaced with high-frequency actuators that directly generate the active blade root pitch. Unlike HHC, an IBC system can generate any waveforms within the bandwidth of the actuators. The IBC test of a full-scale four-bladed BO-105 rotor in the 40- by 80-Foot Wind Tunnel showed 10 dB of noise reduction along with significant vibration reduction using a combination of 2P and 5P blade pitch harmonics (Ref. 17). Note that an HHC system using swashplate oscillation can not generate a 2P input while maintaining a four-bladed rotor intrack. Attempts to duplicate these wind tunnel results in a flight test of the BO-105 helicopter equipped with an IBC system showed noise reduction of more than 5 dBA (Ref. 18). Restricted control authority during the flight test for safety concerns probably limited noise reduction with the IBC system.

Beside the blade root actuation methods using either HHC or IBC, blade-mounted control devices have also shown potential to reduce BVI noise. The test of a model rotor with active trailing edge flaps in the Langley 14- by 22-Foot Subsonic Tunnel showed BVI noise reduction of 4 dB (Ref. 19). The flap schedule for such noise reduction was nonharmonic, being active only for a short azimuth range in the BVI region.

In an effort to develop low-noise, low-vibration tiltrotors, an experiment was conducted at NASA Ames Research Center to evaluate several noise reduction technologies on a full-scale XV-15 rotor in the 80- by 120-Foot Wind Tunnel. The HHC investigation described in this paper is a component of the Short Haul Civil Tiltrotor Program, an element of the Aviation System Capacity Program. The objective was to independently reduce BVI noise and rotor vibratory hub loads. Additional objectives of the test program were to acquire baseline acoustic data at different flight and operating conditions for both three- and four-bladed rotor configurations, and those results are presented in detail in Ref. 20.

Both open-loop and closed-loop results for noise reduction are presented in the paper. Specific findings with regard to HHC effectiveness at different flight conditions and the effects of trim perturbations and control amplitudes on noise reduction are presented. Secondary effects of HHC on the rotor structural loads, vibratory hub loads, and rotor performance are also included. The performance of the vibration controller is also presented.

Test Description

Hardware description

The installation of the XV-15 rotor in the 80- by 120-Foot Wind Tunnel is shown in Fig. 1. The microphone traverse shown in the foreground measures the acoustic footprint under the rotor advancing side. The right-handed rotor of the XV-15 aircraft was mounted on the NASA/Army Rotor Test Apparatus (RTA). The XV-15 rotor is a stiff-inplane hingeless rotor and has a gimballed hub connected to the RTA mast by a Hooke's joint. Test-specific hardware, such as the swashplate, pitch-links, and hub adaptor, were built to allow attachment of the XV-15 rotor to the RTA. Designed as a compromise between the three- and four-bladed hub configurations, the swashplate provided a pitch-link arrangement that generated 29 deg of flap up/pitch up coupling ($\delta_3 = -29$ deg) for the three-blade hub. This δ_3 value is different from that of the XV-15 aircraft, which is –15 deg. Table 1 lists the general rotor properties.

The RTA is a special-purpose test stand for rotor testing and includes an electric-drive motor, right-angle transmission, six-component rotor balance, and both primary and dynamic control systems. The RTA was mounted on a three-strut support system, placing the rotor hub approximately 31 feet (1.24 rotor diameters) above the tunnel floor. The rotor balance measured both steady and vibratory rotor hub loads, including the rotor thrust, drag (H-force), side force, pitching and rolling moments, and shaft torque. For this test, the rotor balance was not calibrated dynamically. The primary control system provided collective and cyclic input for rotor trim.

Table 1. General rotor properties

Number of blades	3
Rotor radius, ft	12.5
Blade chord (constant), in	14.0
Rotor solidity, thrust-weighted, σ	0.089
Blade twist (nonlinear), deg	40.9
Hub precone, deg	1.5
Blade Lock number	3.83
Nominal rotor rpm	589
Hover tip Mach number	0.691

Fig. 1. Isolated XV-15 rotor on the rotor test apparatus in the 80- by 120-Foot Wind Tunnel.

Swashplate excitations

The RTA dynamic control system has three rotary hydraulic actuators located at 0, 180, and 270 deg azimuth under the swashplate to provide 3P excitations. The dynamic control system was locked-out when not in use. Oscillatory 3P excitations from the dynamic control system produced blade pitch harmonics at 2P, 3P, and 4P in the rotating frame, which were superimposed with the trim input from the primary control system. The maximum HHC amplitude was nominally set at 2 deg. However, this magnitude was not reached during the wind tunnel test due to control system load limits under HHC excitation.

Instrumentation

Blade and control system strain gauges were installed at the critical load regions for safety-of-flight monitoring. A bar chart display of structural loads was monitored throughout the test to safeguard against fatigue

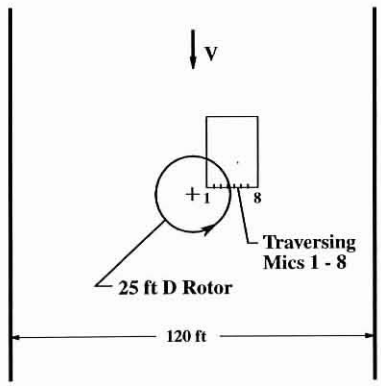

Fig. 2. Microphone locations for the XV-15 test in the 80- by 120-foot test section.

damage to the RTA and rotor system. Since wind tunnel operations limited structural loads within the fatigue levels to ensure infinite life of test components, the operating limits were maintained throughout the test.

Four pairs of dynamic (absolute) pressure transducers were mounted at 65, 78, 85, and 95 percent blade radius. The Kulite transducers were surface-mounted at 5 percent chord from the leading edge, on both upper and lower surfaces at each radial location. The sensor locations were chosen to capture the BVI events and were used as feedback signals for noise control.

The gimbal was instrumented to provide blade flapping angle for trim. A blade pitch transducer, mounted across the pitch bearing, directly measured the trim and HHC input. The rotor balance allowed measurements of both rotor performance and dynamically-uncalibrated vibratory hub loads.

The BVI noise footprint was measured with an acoustic traverse consisting of eight microphones placed 1.8 rotor radii below the advancing side of the rotor disk. Relative to the rotor hub, the traverse microphones spanned 0.36 to 1.69 blade radii in the cross-flow direction and traversed from 0.2 to 2.0 blade radii in the streamwise direction. Figure 2 shows the microphone locations in the test section.

Wind tunnel data acquisition

The wind tunnel data acquisition system has a low-speed and a high-speed chassis. The low-speed chassis acquired rotor performance, loads, and blade response data at 64 samples per-rev for 64 revolutions. The low-speed data were low-pass filtered at 100 Hz before being digitized by the data acquisition system.

High-speed data consisted of microphone and blade pressure signals. These data were low-pass filtered at 4 kHz and sampled at 2048 per-rev for 64 revolutions. The blade-vortex-interaction sound pressure level (BVI-SPL), a measure of BVI noise, was computed by summing all frequency bands in the power spectrum from 10^{th} to 50^{th} blade passage harmonics (approximately 300 to 1500 Hz). This frequency range was selected to highlight the acoustic pulse, the main feature of the BVI event. In addition, the frequency selection prevented the contamination of noise measurements due to reflections at the lower frequencies and background noise at both low and high frequencies (Ref. 21). The wind tunnel test section has a sound-absorbing liner that absorbs more than 90 percent of sound with frequencies higher than 250 Hz. In addition to the liner, sound-absorbing foam was attached to portions of the RTA and selected hard points in the test section to reduce local reflections.

HHC controller

The HHC Controller provided an independent platform for data acquisition, control law execution, and controller output for both open-loop and closed-loop operations. The controller hardware consisted of a Windows-NT PC with a 266 MHz Pentium II processor, a 12-bit, 16 channel National Instruments (NI) AT-MIO-16E-1 data acquisition board, and a 12-bit, 6 channel NI AT-AO-10 board for data output. Dedicated software for HHC operations were developed in-house using Labview. During HHC operations, harmonics of the blade pitch input, instead of swashplate motions, were prescribed at the controller front panel. The controller automatically converted the input harmonics into a swashplate schedule in the collective, longitudinal and lateral cyclic modes. A conversion matrix, precomputed based on a least-squares method, transformed the blade pitch harmonics to harmonics of swashplate motion. Waveforms of swashplate motion were then generated and continuously fed to the output-board to drive the dynamic actuators.

HHC control algorithm

The control algorithm was based on the T-matrix approach, a harmonic control method, for the control of noise and vibration. The HHC plant model was

$$z_n = z_{n-1} + T_n(\theta_n - \theta_{n-1}) \tag{1}$$

where z_n was the controlled vector (or scalar), T_n was the T-matrix, θ_n was the vector of blade pitch harmonics, and n denoted the controller cycle. Depending on the control objectives, each element of the T-matrix represented the sensitivity of a controlled parameter to each harmonic of the blade pitch and was computed using a least-squares method with open-loop data. The controller update cycle was once per rotor revolution. With the plant model, the control law was formulated as an optimization problem:

$$\min\left(z_n^T Q z_n + \theta_n^T R \theta_n\right) \tag{2}$$

where Q and R were diagonal matrices that assigned relative weightings to z_n and θ_n, respectively. The optimal control, including a relaxation factor r ($0 < r < 1$), was:

$$\theta_n = \theta_{n-1} + (1 - r)\, C_n\, z_{n-1} \tag{3}$$

where

$$C_n = -\left(T_n^T Q T_n + R\right)^{-1} T_n^T Q \tag{4}$$

The relaxation factor r was introduced to reduce the controller update rate and to smooth out the output waveforms during controller updates.

Feedback parameters

Different feedback signals were used depending on the controlled parameters. For noise control, both microphone and blade pressure feedback were used independently. The feedback signals were computed in real time during closed-loop operations. For the microphone signals, selected microphones (maximum of four) were sampled at 512 per-rev over four revolutions. The Labview Fast-Fourier-Transform (FFT) routine was employed to compute the spectrum of the microphone signals. The equivalent BVI-SPL, used in the controller, consisted of 10^{th} to 50^{th} blade passage harmonics.

For the noise controller using blade pressure feedback, the controller aimed to reduce a measure of the pressure signals, pre-processed externally before being fed into the controller. The pressure signals were

first bandpass-filtered to highlight the BVI events and then fed into RMS voltmeters to provide a measure of BVI energy. The RMS meter outputs were essentially constants for a test condition. The controller used the rms-pressure signals, sampled at 128 per-rev and averaged over four revolutions, as the feedback for noise control.

For vibration, the controller used signals from the rotor hub loads-thrust, H-force, side force, and pitching and rolling moments. The 3P hub load components were extracted from the signals using a Labview FFT routine. The objective of the controller was to suppress the vibration index, a weighted-measure of the root-mean-square of the 3P hub load harmonics. To render all quantities with the same dimension, the hub moments (in ft-lb) were normalized by the rotor radius in the computation of the vibration index.

Test conditions

The test conditions for HHC investigation are shown in Table 2. A test condition was set to advance ratio μ, rotor loading C_T/σ, and shaft tilt α (positive values for rearward tilt). Unless specified otherwise, zero one-per-rev flapping was maintained during the test conditions. Therefore, the equivalent tip-path-plane angle of attack, based on the gimbal flapping angle, was equal to the shaft tilt angle. Since the tip Mach number was known to have a major effect on the noise level, it was strictly maintained at 0.691 at all noise-related test conditions.

Results and Discussion

Control of BVI noise

The effects of HHC on BVI noise were evaluated at four simulated landing approach conditions of the XV-15 tiltrotor aircraft as shown in Table 2. The maximum BVI noise condition in the table is the first condition listed: 0.17 advance ratio, 0.09 C_T/σ, and 3 deg rearward shaft tilt.

Open-loop phase sweeps. Open-loop phase sweeps using individual 2P, 3P, 4P components of blade pitch were initially performed to explore the behavior of BVI noise under HHC excitation. These preliminary results were also used to assess vibratory hub loads and rotor structural loads during HHC application and allowed an evaluation of the signal processing techniques of blade pressure for closed-loop operations for noise control. The HHC amplitude was selected to remain uniform throughout the phase sweep while keeping the structural loads within the operating limits. The rotor was not retrimmed during the phase sweep. The BVI noise was measured with the microphone traverse parked at a location slightly ahead of the rotor disc. The BVI-Sound Pressure Level (BVI-SPL) shown in subsequent figures was the highest level measured by any one of the eight traverse microphones. Therefore, a directivity change that moved the peak noise to a different microphone would not appear as a noise reduction even though the noise at a specific microphone location had been reduced.

Table 2. HHC test conditions

Test Conditions			Primary objectives			
			BVI Noise			
				Closed-loop		
μ	C_T/σ	α, deg (pos. aft)	Open-loop	Mic	Pressure	Vibration
0.170	.090	3	X		X	
0.150	.090	3	X	X	X	
0.150	.090	0	X		X	
0.150	.090	−3	X		X	
0.125	.090	−2				X
0.170	.090	−5				X

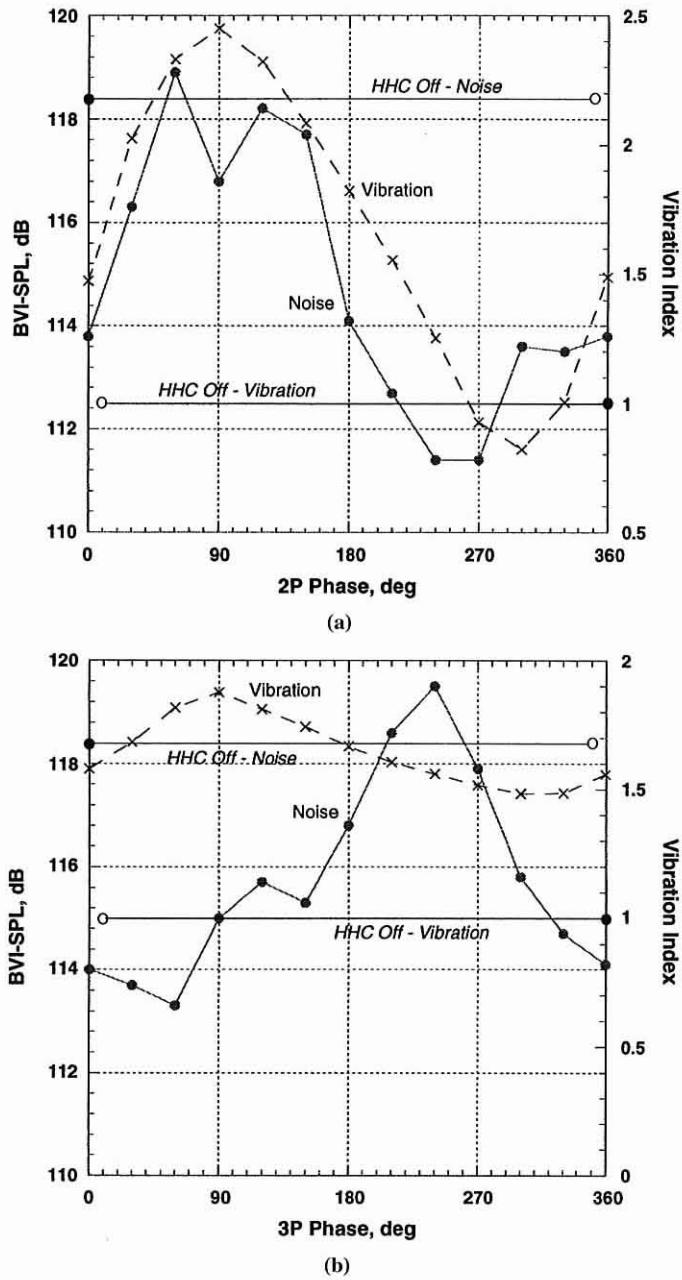

Fig. 3. Variation of BVI noise and 3P hub loads with HHC phase, (a) 2P sweep, 1.4 deg amplitude, (b) 3P sweep, 0.7 deg amplitude. μ = 0.15, C_T/σ = 0.09, α = 3 deg aft.

The open-loop phase sweep using 2P and 3P input are shown in Fig. 3 for the test condition of 0.15 advance ratio, 0.09 C_T/σ, and 3 deg rearward shaft tilt. Figure 3(a) shows the results for the 2P phase sweep with 1.4 deg amplitude. The 2P input is quite effective in reducing BVI noise at this test condition. Noise reduction was achieved at nearly all input phases, except at 60 deg where the noise was increased slightly. The results in the 270 deg phase region suggest that noise reduction in excess of 7 dB can be achieved using 2P input alone. The vibration index, defined as

the root-mean-square of the five 3P hub load harmonics, was normalized to 1 for the HHC-Off case. The vibration index was also reduced in the phase region of minimum noise, particularly at 300 deg phase where it was reduced by about 20 percent. As mentioned previously, the rotor balance was not calibrated dynamically, and thus, the vibration index was not intended to be a precise measurement, but was useful as a general indication of the vibration level.

The 3P HHC phase sweep results are shown in Fig. 3(b). Due to high control loads, the 3P amplitude was limited to 0.7 deg or one-half of the 2P amplitude. The two structural components reaching operating limits during HHC operations were the pitch-link and the primary actuators. Since not all harmonics of the pitch-link loads were transferred to the actuators in the fixed-system, each of these two structural components was more sensitive to certain input harmonics than to others. For this phase sweep, the best noise reduction of 5.1 dB was achieved at 60 deg 3P phase. At this input phase, a significant increase in the 3P normal force caused an 80 percent increase in the vibration index from the baseline level. In fact, the vibration was increased at all phases of 3P input.

Note that the noise reduction results shown in Fig. 3(a) are similar to those reported in Ref. 22 for an IBC test of a four-bladed, full-scale BO-105 rotor in the NASA Ames 40- by 80-Foot Wind Tunnel. The noise variations with the 2P input phase sweep of the XV-15 and the BO-105 rotors are shown in Fig. 4. The BO-105 was tested at a high BVI noise condition ($\mu = 0.15$, $C_T/\sigma = 0.07$, $\alpha = 2.9$ deg aft), and the noise results were obtained from a single microphone at the peak noise location (0.76 blade radius, 133 deg azimuth, and 1.17 radius below the hub plane). Figure 4 shows that both phase sweep results display two local minima for noise, one in the 90 deg phase region and the other at 270 deg, where the BVI noise levels are reduced by 7 dB in both rotor tests.

With regards to rotor structural loads, the XV-15 test results show that HHC has negligible effects on the steady components but significant effects on the alternating components. Figure 5 shows the effects of 2P input on the half peak-to-peak values of the blade flap and chord bending moments at 35 percent radius and pitch-link load. The test condition was identical to that of Fig. 3(a). The 2P input had moderate effects on the alternating blade bending moments and, in fact, showed beneficial effects at the phase region of 270 deg for minimum noise. However, the

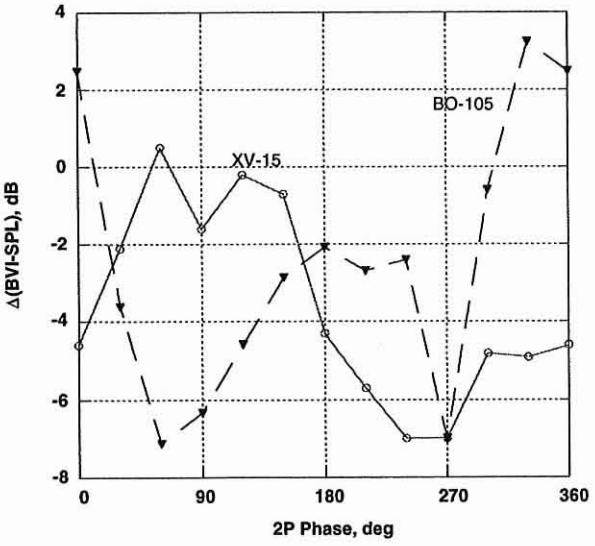

Fig. 4. Variation of BVI noise with 2P HHC phase at $\mu = 0.15$ for the XV-15 ($C_T/\sigma = 0.09$, $\alpha = 3$ deg aft) and BO-105 rotors ($C_T/\sigma = 0.07$, $\alpha = 2.9$ deg aft).

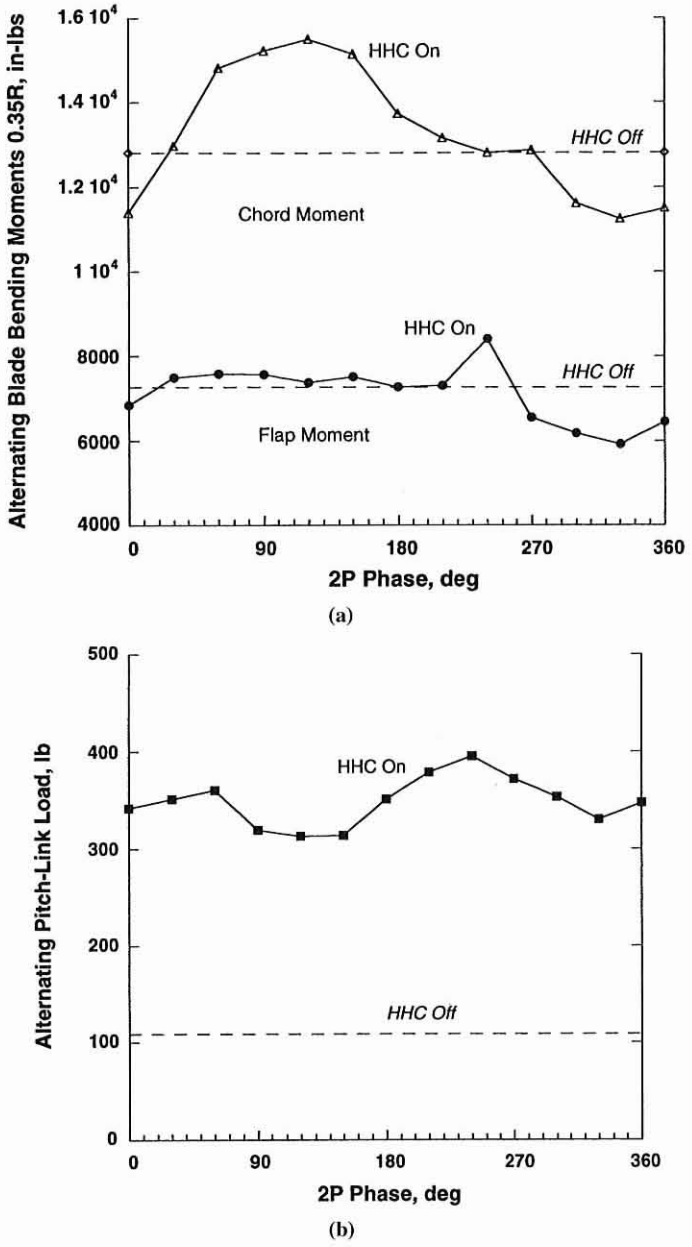

Fig. 5. Variation of alternating (a) blade bending moments and (b) pitch-link load with 2P HHC phase, 1.4 deg amplitude. $\mu = 0.15$, $C_T/\sigma = 0.09$, $\alpha = 3$ deg aft.

alternating pitch-link load was increased by a factor of 3 to 4 with 2P excitations.

An evaluation of the rms-pressure signal for identification of BVI noise is shown in Fig. 6. The baseline test condition was a high BVI noise condition at 0.17 advance ratio, 0.09 C_T/σ, and 3 deg rearward shaft tilt. Phase sweeps with 2P are shown in Fig. 6(a) and 4P in Fig. 6(b). Nominal amplitudes were 1.4 deg for the 2P and 0.7 deg for the 4P input. For the 2P case, BVI noise was reduced at all input phases, with a maximum reduction of 5.1 dB at 260 deg phase. The rms-pressure signal from the Kulite at 85 percent blade station agrees reasonably well with noise under 2P excitations. The agreement is particularly good at the phase region of minimum noise, a very encouraging fact for closed-loop operations. However, the 4P phase sweep results shown in Fig. 6(b) reveal a different trend. The 4P phase for minimum noise at 150 deg (3.8 dB reduction)

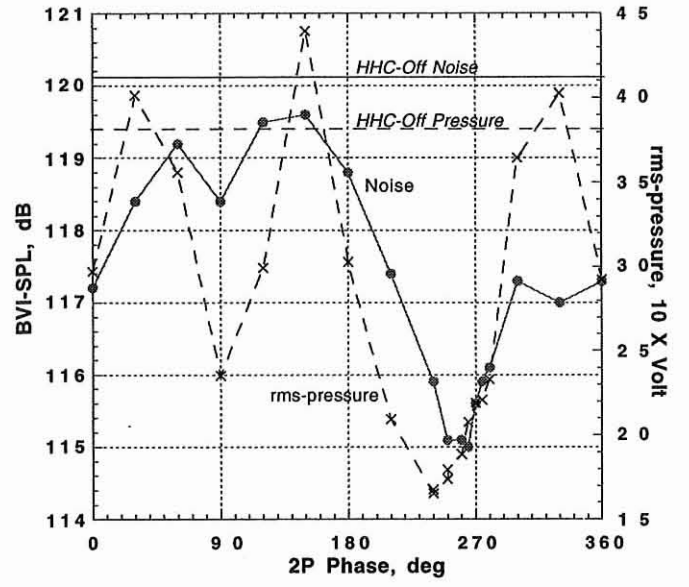

(a)

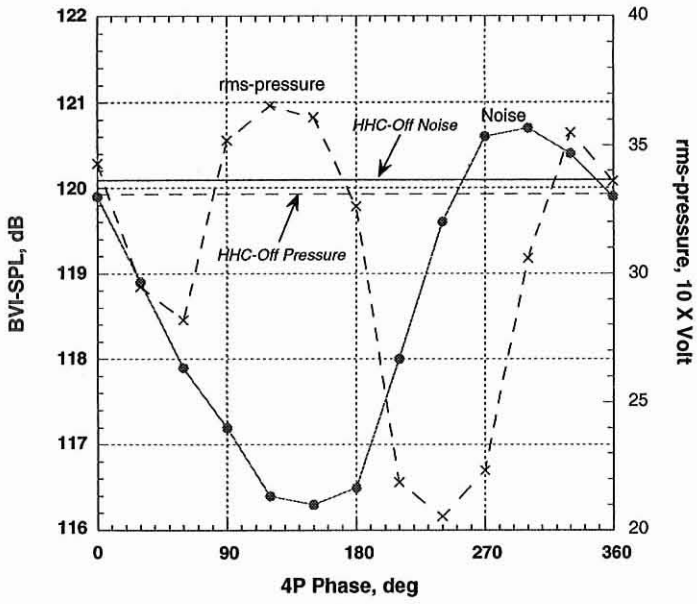

(b)

Fig. 6. Variation of BVI noise and rms-pressure signal at 0.85R with (a) 2P HHC phase, 1.4 deg amplitude, and (b) 4P HHC phase, 0.7 deg amplitude. $\mu = 0.17$, $C_T/\sigma = 0.09$, $\alpha = 3$ deg aft.

was close to the phase of a local maximum in the rms-pressure signal. A negative correlation between BVI noise and rms-pressure was also observed with the 3P phase sweep (not shown) at the phase of minimum noise.

The inboard pressure transducers at 0.65 and 0.78 radial stations failed during the wind tunnel test. The pressure signal at 95 percent blade radius did not correlate well with the noise levels. A post-test free wake analysis showed that the signal was contaminated with multiple perpendicular BVI events in the 90 deg azimuth region. Since perpendicular interactions do not contribute significantly to BVI, pressure measurements near the blade tip region are not useful for noise identification.

Open-loop amplitude sweep. Amplitude sweeps were conducted at the optimum phase of each of the HHC harmonics shown in Fig. 6. The

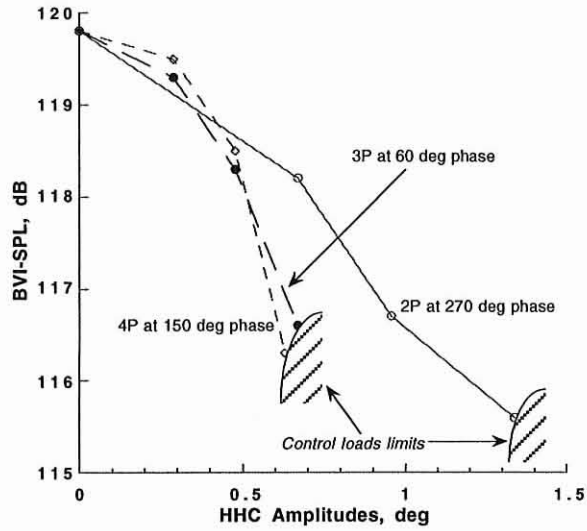

Fig. 7. Variation of BVI noise with HHC amplitude at phases of best noise reduction. $\mu = 0.17$, $C_T/\sigma = 0.09$, $\alpha = 3$ deg aft.

corresponding results are shown in Fig. 7 (0.17 advance ratio, 0.09 C_T/σ, and 3 deg rearward shaft tilt). For each of the optimal input phases—270 deg for 2P, 60 deg for 3P, and 150 deg for 4P input—the amplitudes were increased incrementally until the control loads reached 95 percent of operating limits. Among the three input harmonics, the 2P obtained the largest noise reduction simply because the control loads were least sensitive to this input component. At the load limits, the 2P amplitude was close to 1.4 deg, while the allowable amplitudes for both 3P and 4P components were less than 0.7 deg. For this test condition, the 4P input was the most efficient and the 2P least efficient in terms of noise reduction level per deg of HHC. The noise levels varied quadratically with the 3P and 4P amplitudes.

The blade pitch schedules generated using the optimal phase angles shown in Fig. 7 reveal that each of the three schedules has a maximum blade pitch near 135 deg azimuth, the region where the BVI-dominant vortex forms. Tiltrotors have a unique behavior with regards to the formation of the trailed vortices. The high twist of tiltrotor blades shifts the lift distribution inboard sufficiently to generate a negative tip loading over the advancing side of the rotor disk in some flight conditions. The loading reversal in turn generates a pair of counter-rotating vortices, as shown with flow-visualizations of a small-scale V-22 rotor tested in a descent flight condition (Ref. 23). Some noise reductions achieved in the current investigation were probably caused by either a mutual-interference of the vortex-pair before interacting with the blades or a weakening of the inboard vortex. Furthermore, since the 2P schedule has a minimum pitch at 45 deg azimuth, in the advancing BVI region, reduction in blade loading during interaction is the probable mechanism for noise reduction in this case. Finally, even though test results yield no information about the wake geometry, increases in blade-vortex miss distance is also a potential mechanism for noise reduction.

Effects of test condition. The effect of airspeed on noise reduction with HHC is shown in Fig. 8 using the 2P phase sweep data. The two test conditions shown in the figure differ only in airspeed (0.15 vs. 0.17 advance ratio), both having the same C_T/σ of 0.09 and 3 deg rearward shaft tilt. The nominal 2P amplitude was 1.4 deg for both cases. Since these test conditions had different baseline noise levels, the results are presented in terms of changes in the noise level, or Δ(BVI-SPL), from their respective baseline levels. In particular, the low speed case has a

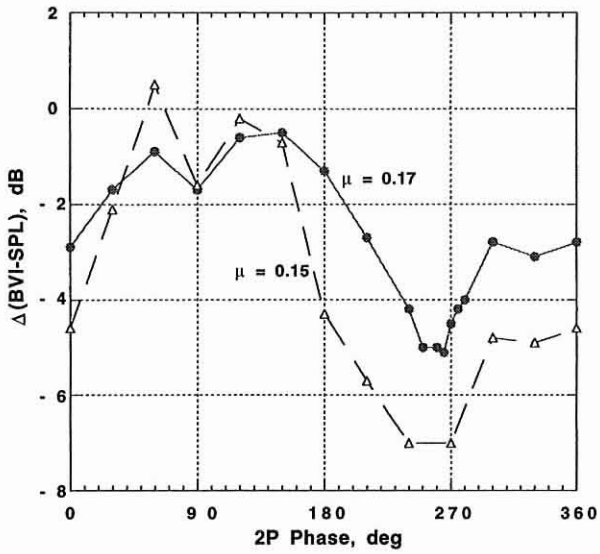

Fig. 8. Variation of BVI noise with 2P HHC phase, 1.4 deg amplitude, at two advance ratios. $C_T/\sigma = 0.09$, $\alpha = 3$ deg aft.

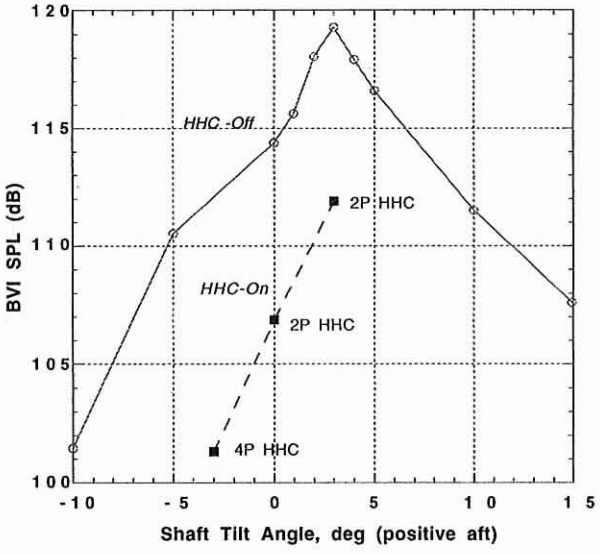

Fig. 9. BVI noise reduction with HHC at different rotor shaft angles. $\mu = 0.15$, $C_T/\sigma = 0.09$.

lower baseline noise than the higher speed case, 118.4 dB vs. 120.1 dB. The overall variations of noise with 2P phase are similar between the two test conditions. However, the condition with the lower baseline noise level (0.15 advance ratio) had a larger noise reduction, 7.1 dB vs. 5.1 dB. Similar results were obtained from the 3P and 4P phase sweeps at the low speed case ($\mu = 0.15$).

An investigation of shaft tilt effects on noise reduction with HHC was conducted to determine whether the benefits of HHC and low-noise flight operations were additive. Open-loop HHC was applied at two additional shaft angles, 0 deg and 3 deg forward tilt, both at 0.15 advance ratio and 0.09 C_T/σ. Compared to the peak BVI noise condition at 3 deg rearward shaft tilt, the 0 deg and 3 deg forward shaft tilt conditions are lower noise. All three test conditions with HHC are within the landing approach profiles of the XV-15 aircraft. The summary results, presented in Fig. 9, show the noise variation with shaft tilt angle both with and without HHC. The HHC data were the best noise reductions obtained at the test conditions. In particular, optimal noise reduction results at 0 and 3 deg shaft angles were achieved with 1.4 deg of 2P input, while the large noise reduction at −3 deg shaft tilt (forward) was achieved with 0.7 deg of 4P input. The results show that HHC is even more effective in reducing noise at a lower BVI noise condition, almost doubling the 7 dB reduction level achieved at the higher noise condition. HHC application at a lower noise condition yielded a total noise reduction of 16.5 dB from the peak uncontrolled noise level. These results suggest that HHC should best be used in combination with flight operations for low-noise approach to amplify its effectiveness.

Reduction in the noise footprint. The acoustic traverse was exercised to quantify the BVI directivity with HHC and to determine whether noise reduction was achieved over the entire acoustic footprint. Figure 10 shows the acoustic footprints with HHC on and off for the 3 deg forward shaft tilt condition (0.15 advance ratio and 0.09 C_T/σ) shown in Fig. 9. The 4P HHC amplitude was 0.7 deg. For the traverse results, the rotor was typically retrimmed after HHC application to match the baseline trim conditions. Since the rotor trim states were not affected by the 4P input, no retrimming was necessary in this case. The peak noise levels are located at the upper left corners of the traverse area for both cases, and the baseline peak (HHC-Off) is 114.0 dB. With HHC-On, the peak noise level is 102.0 dB, a 12.0 dB reduction in the peak noise level. Noise reduction level over the acoustic footprint was not uniform, varying from 4.2 dB to 13.6 dB. The largest noise reduction occurred in the high noise region of the baseline case.

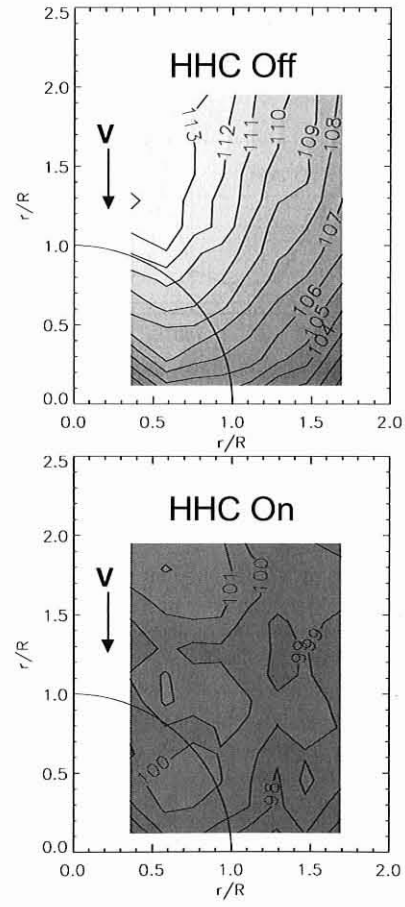

Fig. 10. Noise reduction with 4P HHC over BVI-SPL contour. $\mu = 0.15$, $C_T/\sigma = 0.09$, $\alpha = 3$ deg forward.

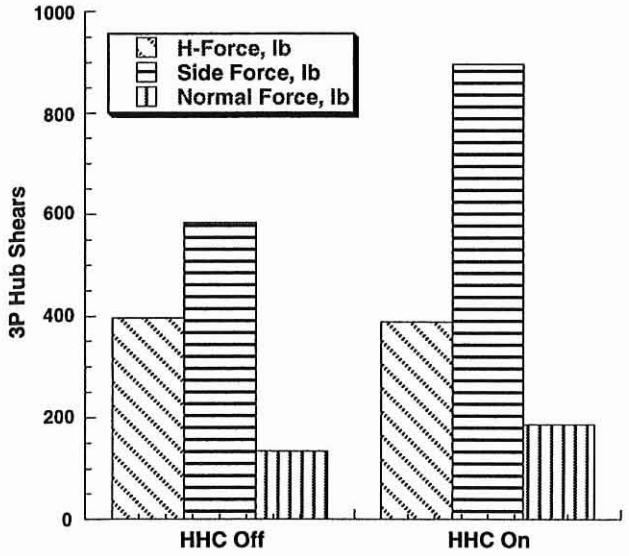

Fig. 11. Effect of 4P HHC for noise reduction on 3P hub loads. μ = 0.15, C_T/σ = 0.09, α = 3 deg forward.

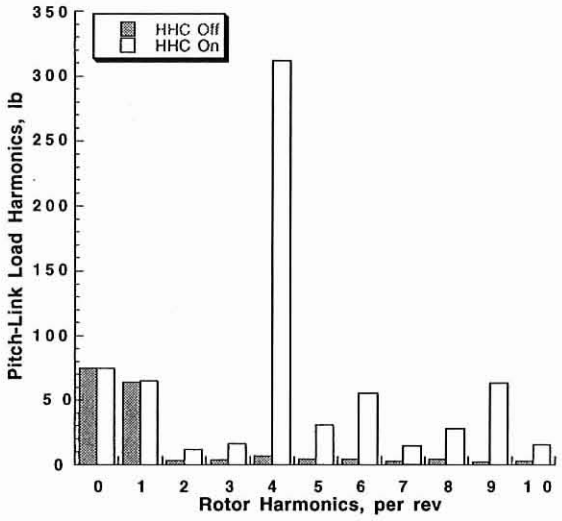

Fig. 12. Effect of 4P HHC for noise reduction on harmonics of pitch-link load. μ = 0.15, C_T/σ = 0.09, α = 3 deg forward.

For the noise reduction result shown in Fig. 10, HHC input had a moderate effect on the vibratory hub loads, a significant effect on the control system loads, and a negligible effect on rotor performance. The effects of 4P input on the measured 3P hub shears are shown in Fig. 11. The 4P input slightly reduced the H-force and moderately increased the side and normal forces. The alternating pitch-link load was increased by a factor of 4.5, and the harmonics of this load component are shown in Fig. 12. The 4P input caused a significant increase in the 4P component of the alternating pitch-link load, dominating increases in all other harmonics. The sixth and ninth harmonics of the pitch-link load increased moderately with HHC, while the steady and the 1P component were unaffected. Even though the control system hardware used in the tunnel installation are different from that of the XV-15 aircraft, these results imply that blade torsion dynamics could be an important consideration in the application of HHC to rotorcraft.

The effects of 4P input on rotor power were small. The equivalent rotor power, a measure of power at constant propulsive force, was increased by

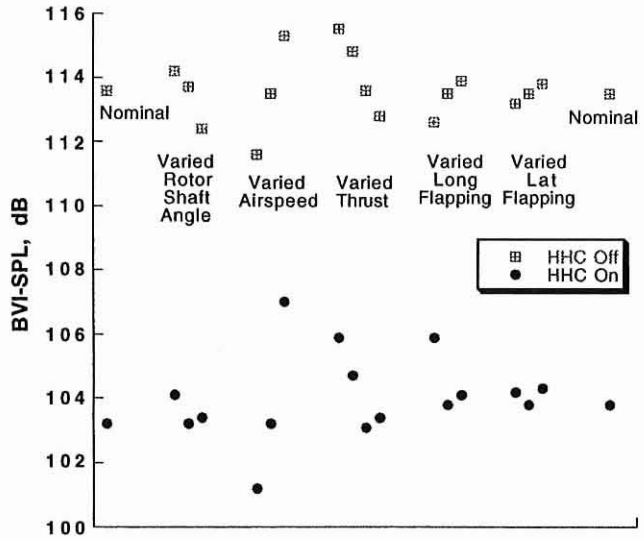

Fig. 13. Effects of trim and flight condition perturbations (increasing left to right) on BVI noise reduction with HHC. Baseline condition: μ = 0.15, C_T/σ = 0.09, α = 3 deg forward.

1 percent. This increase includes changes in rotor shaft power and rotor drag. Because these approach flight conditions were already at low shaft power and occupy only a small portion of the flight envelope, increases of this magnitude were not a concern.

Effects of trim perturbations on noise reduction. The effects of changing test conditions and trim parameters on the noise reduction results of Fig. 10 were evaluated. For this investigation, the acoustic traverse was parked at the upstream end of the traverse area to capture the peak noise levels. The same 4P input (0.7 deg amplitude) was turned on and off while the shaft angle, advance ratio, rotor thrust, longitudinal and lateral flapping were varied independently. Shaft angle and flapping perturbations were ± 1 deg, advance ratio was varied by ± 5 percent, and rotor thrust was perturbed from -10 to $+5$ percent in 5 percent increments. The results are shown in Fig. 13. The HHC-Off baseline noise level was sensitive to shaft tilt, airspeed, rotor thrust, and longitudinal flapping and less sensitive to lateral flapping. The results with HHC showed that noise reductions remained robust with these perturbations, achieving more than 9 dB reduction in most cases. Even for the worst case with a perturbation in longitudinal flapping, the reduction level was nearly 7 dB.

Closed-loop results. Closed-loop noise control was tested with different combinations of feedback signals and HHC input harmonics. Microphone feedback yielded results similar to the open-loop results. The noise reduction achieved with the controller using blade pressure feedback and only 2P input is shown in Fig. 14. As with the open-loop cases, the noise controller was limited by control loads. The HHC amplitudes were not constrained explicitly in the controller but were limited manually by monitoring the control system structural limits. The baseline test condition was a high noise condition (0.15 advance ratio, 0.09 C_T/σ, and 3 deg rearward shaft tilt). The rotor was retrimmed after the controller had reached a steady-state value. The peak noise levels occurred slightly to the lower left of the traverse center in both cases. The peak-to-peak reduction is 5.3 dB, 1.6 dB less than that achieved with the open-loop 2P traverse (contour of BVI-SPL not shown). The small degradation in noise reduction with the controller suggests the signal processing technique used for blade pressure feedback requires additional refinement.

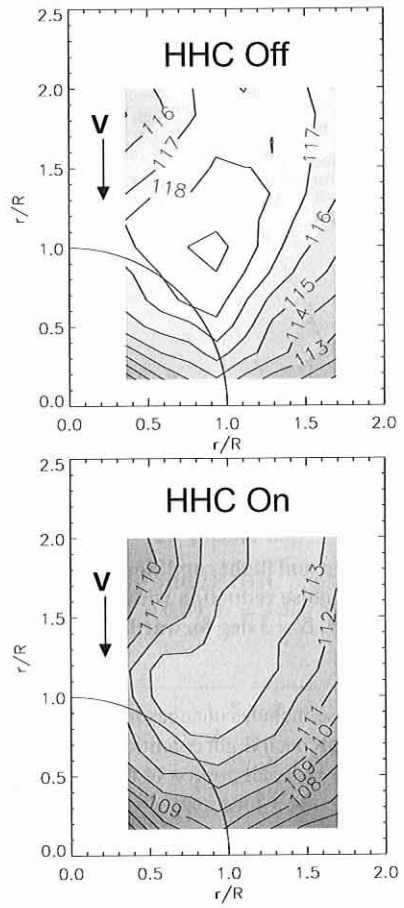

Fig. 14. Noise reduction with blade pressure feedback controller over BVI-SPL contour. $\mu = 0.15$, $C_T/\sigma = 0.09$, $\alpha = 3$ deg aft.

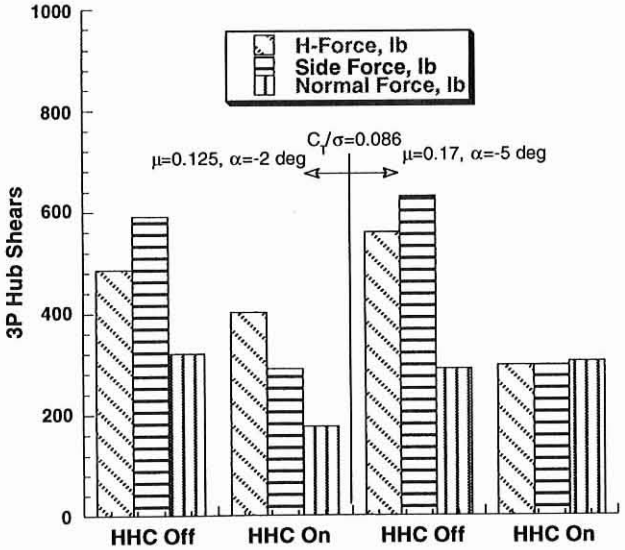

Fig. 15. Reduction in 3P hub loads with the vibration controller at two forward flight conditions.

Control of rotor vibratory hub loads

The vibration controller was tested at two forward flight conditions to evaluate the capability of multi-harmonic input, consisting of 2P, 3P, 4P, to reduce the 3P hub loads on the XV-15 rotor. In both cases, the T-matrices were identified off-line using open-loop data. Figure 15 shows that the controller achieves simultaneous 3P hub loads reduction at both test conditions. The controller reduced the vibration indices by 34 percent at the low speed and 52 percent at the high speed. For the lower speed case, the side and normal forces were reduced by roughly half, while the H-force was reduced only slightly. For the higher speed, all hub load components except for the normal force were reduced by more than half. As with the noise controller, the HHC amplitudes were manually limited by monitoring the structural loads limits. The increases in control system loads, reaching the operating limits, precluded the HHC authority necessary for further reduction. The root-mean-square values of HHC input for both cases were close to 0.9 deg (0.91 deg for μ of 0.125 and 0.87 deg for μ of 0.17).

Concluding Remarks

Higher harmonic control was applied to a full-scale, isolated three-bladed XV-15 rotor in the NASA Ames 80- by 120- Foot Wind Tunnel to independently control blade-vortex interaction noise and rotor vibratory hub loads. The higher harmonic blade pitch 2P, 3P, 4P was generated using swashplate excitation. The radiated blade-vortex interaction (BVI) noise was measured on a plane beneath the rotor with eight microphones mounted on an acoustic traverse. Specific findings are:

1) HHC was very effective in reducing BVI noise on the XV-15 rotor, achieving up to 12 dB in noise reduction.

2) The noise controller using blade pressure feedback successfully reduced BVI noise.

3) HHC was more effective for noise reduction at the lower BVI noise conditions.

4) BVI noise reduction with open loop HHC was robust to perturbations in rotor trim and test condition.

5) BVI noise reduction level varied quadratically with HHC 3P and 4P amplitudes and almost linearly with 2P amplitude. The 4P input was the most efficient in terms of noise reduction level per input degree.

6) BVI noise reduction with HHC was limited by increases in control loads.

7) HHC effects on blade bending moments and rotor performance were small.

8) BVI noise reduction with HHC either increased or decreased 3P hub loads depending on the harmonics.

9) The vibration controller showed potential to reduce vibratory hub loads on the XV-15 rotor in helicopter mode; increases in control load prevented larger reductions.

References

[1]"Civil Tiltrotor Mission and Application, Phase II: The Commercial Passenger Market," NASA CR 177576, February 1991.

[2]Nguyen, K., and Chopra, I., "Application of Higher Harmonic Control to Hingeless Rotor Systems," *Vertica*, Vol. 14, (4), 1990.

[3]Schmitz, F., and Yu, Y, "Helicopter Impulsive Noise: Theoretical and Experimental Status," *Journal of Sound and Vibration*, Vol. 109, (3), 1986.

[4]Johnson, W., *Helicopter Theory*, Princeton University Press, 1980.

[5]Prieur, J., and Splettstoesser, W., "ERATO—an ONERA-DLR Cooperative Programme on Aeroacoustic Rotor Optimisation," Paper No.

B6, 25th European Rotorcraft Forum, Rome, Italy, September 14–16, 1999.

[6]Conner, D., Marcolini, M., Decker, W., Cline, J., Edwards, B., Nicks, C., and Klein, P., "XV-15 Tiltrotor Low Noise Approach Operations," American Helicopter Society 55th Annual Forum Proceedings, Montreal, Canada, May 25–27, 1999.

[7]Brooks, T., and Booth, E., "The Effects of Higher Harmonic Control on Blade-Vortex Interaction Noise and Vibration," *Journal of the American Helicopter Society*, Vol. 35, (3), July 1993.

[8]Splettstoesser, W., Schultz, K., Kube, R., Brooks, T., Booth, E., Niesl, G., and Streby, O., "A Higher Harmonic Control Test in the DNW to Reduce Impulsive BVI Noise," *Journal of the American Helicopter Society*, Vol. 39, (4), Oct 1994.

[9]Splettstoesser, W., Kube, R., Wagner, W., Seelhorst, U., Boutier, A., Micheli, F., Mercker, E., and Pengel, K., "Key Results from a Higher Harmonic Control Aeroacoustic Rotor Test (HART) in the German-Dutch Wind Tunnel," *Journal of the American Helicopter Society*, Vol. 42, (1), Jan 1997.

[10]Polychroniadis, M., "Generalized Higher Harmonic Control—Ten Years of Aerospatiale Experience," Paper No. III.7.2, Sixteenth European Rotorcraft Forum, Glasgow, Scotland, September 18–20, 1990.

[11]Wood, E., Powers, R., Cline, J., and Hammond, C., "On Developing and Flight Testing a Higher Harmonic Control System," *Journal of the American Helicopter Society*, Vol. 30, (1), January 1985.

[12]Miao, W., Kottapalli, S., and Frye, H., "Flight Demonstration of Higher Harmonic Control on the S-76 Rotor," American Helicopter Society 42nd Annual Forum Proceedings, Washington, D.C., June 2–4, 1986.

[13]Polychroniadis, M., and Achache, M., "Higher Harmonic Control: Flight Test on a SA 349 Research Gazelle," American Helicopter Society 42nd Annual Forum Proceedings, Washington, D.C., June 2–4, 1986.

[14]Hammond, C., "Wind Tunnel Results Showing Rotor Vibratory Loads Reduction Using Higher Harmonic Blade Pitch," *Journal of the American Helicopter Society*, Vol. 28, (1), January 1983.

[15]Shaw, J., Albion, N., Hanker, E., and Teal, R., "Higher Harmonic Control: Wind Tunnel Demonstration of Fully Effective Vibratory Hub Force Suppression," *Journal of the American Helicopter Society*, Vol. 34, (1), January 1989.

[16]Nixon, M., Kvaternik, R., and Settle, B., "Tiltrotor Vibration Reduction through Higher Harmonic Control," American Helicopter Society 53rd Annual Forum Proceedings, Virginia Beach, VA, April 29–May 1, 1997.

[17]Swanson, S., Jacklin, S., Blaas, A., Niesl, G., and Kube, R., "Acoustic Results from a Full-Scale Wind Tunnel Test Evaluating Individual Blade Control," American Helicopter Society 51st Annual Forum Proceedings, Ft. Worth, TX, May 9–11, 1995.

[18]Splettstoesser, W., Schultz, K., van der Wall, B., Buchholz, H., Gembler, W., and Niesl, G., "The Effect of Individual Blade Pitch Control on BVI Noise—Comparison of Flight Test and Simulation Results," Paper No. AC07, 24th European Rotorcraft Forum, Marseilles, France, September 15–17, 1998.

[19]Marcolini, M., Booth, E., Tadghighi, H., Hassan, A., Smith, C., and Becker, L., "Control of BVI Noise Using an Active Trailing Edge Flap," American Helicopter Society 1995 Vertical Lift Aircraft Design Conference, San Francisco, CA, January 18–20, 1995.

[20]Kitaplioglu, C., Betzina, M., and Johnson, W., "Blade-Vortex Interaction Noise of an Isolated Full-Scale XV-15 Tilt-Rotor," American Helicopter Society 56th Annual Forum Proceedings, Virginia Beach, VA, May 2–4, 2000.

[21]Kitaplioglu, C., McCluer, M., and Acree, C., "Comparison of XV-15 Full-Scale Wind Tunnel and In-Flight Blade-Vortex Interaction Noise," American Helicopter Society 53rd Annual Forum Proceedings, Virginia Beach, VA, April 29–May 1, 1997.

[22]Jacklin, S., Nguyen, K., Blass, A., and Richter, P., "Full-Scale Wind Tunnel Test of a Helicopter Individual Blade Control (IBC) System," American Helicopter Society 50th Annual Forum Proceedings, Washington, D.C., May 11–13, 1994.

[23]Yamauchi, G., Burley, C., Mercker, E., Pengel, K., and JanakiRam, R., "Flows Measurements of an Isolated Model Tilt Rotor," American Helicopter Society 55th Annual Forum Proceedings, Montreal, Canada, May 25–27, 1999.